Journal of Photochemistry and Photobiology A: Chemistry 205 (2009) 98–103

Contents lists available at ScienceDirect

Journal of Photochemistry and Photobiology A: Chemistry

journal homepage: www.elsevier.com/locate/jphotochem

Comparing electroluminescence efficiency and photoluminescence quantum yield of fluorene-based π-conjugated copolymers with narrow band-gap comonomers

Jungwook Han[a], Jongdeok An[a], Chan Im[a,c,*], Nam Sung Cho[b], Hong Koo Shim[b], Tetsuro Majima[c]

[a] Department of Chemistry, Konkuk University, 1 Hwayang-dong, Gwangjin-gu, Seoul 143-701, Republic of Korea
[b] Department of Chemistry and School of Molecular Science (BK21), Korea Advanced Institute of Science and Technology, 373-1 Guseong-dong, Yuseong-gu, Daejeon 305-701, Republic of Korea
[c] The Institute of Scientific and Industrial Research (SANKEN), Osaka University, Mihogaoka 8-1, Ibaraki, Osaka 567-0047, Japan

ARTICLE INFO

Article history:
Received 8 October 2008
Received in revised form
26 December 2008
Accepted 13 February 2009
Available online 3 May 2009

Keywords:
π-Conjugated copolymer
OLED
Photoluminescence
Electroluminescence
Energy transfer

ABSTRACT

Recent interest in π-conjugated statistical copolymers, as well as their analog alternating copolymer, is due to their relatively high efficiencies as red light-emitting diodes and photovoltaic cells when used as active semiconductors. An example of this type of copolymer is poly{9,9-bis(2′-ethylhexyl)fluorene-2,7-diyl-co-2,5-bis(2-thienyl-1-cyanovinyl)-1-(2′-ethylhexyloxy)-4-methoxybenzene-5″,5‴-diyl}, which is synthesized from monomers 2,7-dibromo-9,9-bis(2′-ethylhexyl)fluorene and 2,5-bis(2-(5′-bromothienyl)-1-cyanovinyl)-1-(2″-ethylhexyloxy)-4-methoxybenzene. Accordingly, this study investigates the exciton dynamics of these materials as model copolymeric systems at systematically varied comonomer ratios. For a more quantitative exploration of the copolymer systems more quantitatively, ultraviolet–visible absorption and photoluminescence spectroscopy were utilized for diluted solutions and spin-cast thin films. The photoluminescence quantum yield was calculated from the time-integrated spectroscopic data. The yield values are discussed in terms of a primary kinetics model and used to clarify the different exciton dissipation behaviors of solutions and films. Moreover, the fundamental data are compared with previously reported electroluminescence efficiencies.

1. Introduction

Ever since Friend et al. showed that a soluble π-conjugated polymer could be used as a promising active semiconductor for a light-emitting diode (LED) application [1], soluble π-conjugated polymers have attracted an extraordinary amount of attention due to their unique properties [2,3]. Copolymerization has subsequently become one of the most important synthetic means of modifying the physical and chemical properties of polymers [4,5].

A unique advantage of copolymerization is its ability to form strong covalent bonds between different types of monomers with functionalities that offset each other. In contrast, physically blended systems, such as a polymer film doped with small molecules, can experience unavoidable phase-separation problems, especially for a device operating in an external electric field. There have been many partially successful improvements to device performance via copolymerization. Nonetheless, there is still a problem of sparse predictability in the design of optimum copolymers with a minimum of unexpected effects that can result from the incorporation of different functionalities.

A series of copolymers introduced by Shim et al. demonstrate the typical competitive interplay between, for instance, radiative and non-radiative dissipation of photo-generated excitons upon the incorporation of comonomers with a narrow band-gap into a blue-emitting fluorene-based polymer chain [6]. These copolymers also have an interesting aspect in terms of their application because they can be used as red-emitting materials for LED applications and as photo-receptive materials for photovoltaic cell applications.

Poly{9,9-bis(2′-ethylhexyl)fluorene-2,7-diyl-co-2,5-bis(2-thienyl-1-cyanovinyl)-1-(2′-ethylhexyloxy)-4-methoxybenzene-5″,5‴-diyl} (PFTCVBxs) shown in Fig. 1 were originally synthesized to control the way colors are emitted. In fact, these copolymers can be used successfully as red-emitting materials in polymer LEDs. For this purpose, they utilize incorporated monomers with a narrow band-gap, 2,5-bis(2-(thienyl)-1-cyanovinyl)-1-(2″-ethylhexyloxy)-4-methoxybenzene (TCVB), on fluorene-based polymer chains consisting of 9,9-bis(2′-ethylhexyl)fluorene (EHF) monomers. Shim and co-workers [7] also synthesized an alternating copolymer (PFR3-S) with the same comonomers used with

* Corresponding author at: Department of Chemistry, Konkuk University, 1 Hwayang-dong, Gwangjin-gu, Seoul 143-701, Republic of Korea. Tel.: +82 2 450 3415; fax: +82 2 3436 5382.
E-mail address: chanim@konkuk.ac.kr (C. Im).

1010-6030/$ – see front matter © 2009 Elsevier B.V. All rights reserved.
doi:10.1016/j.jphotochem.2009.02.020

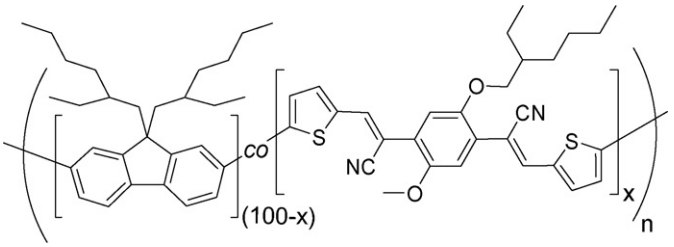

Fig. 1. Chemical structure of PFTCVB*x*.

PFTCVB*x*s. This alternating copolymer, PFR3-S, can also be used as a red-emitting material for a polymer LED.

The alternating copolymer is reportedly useful for photovoltaic cells as an active semiconductor [8]. A power conversion efficiency of approximately 1% under AM1.5 (100 mW/cm^2) can be achieved with the aid of PFR3-S and a fullerene blend system. Interestingly, Koetse et al. [9] used this copolymer for a polymer:polymer blended photovoltaic cell and showed that it is possible to achieve a power conversion efficiency of approximately 1.5%.

This study explores these copolymers as model systems. By understanding their photo-generated exciton decay characteristics when the TCVB unit ratio is quantitatively increased, we can connect these characteristics to appropriate optoelectronic properties in devices. To this end, we carefully conducted time-integrated ultraviolet–visible (UV–vis) absorption and photoluminescence (PL) spectroscopic studies on a diluted solution and on thin film samples as a function of the TCVB concentration. The resulting data were converted into PL quantum yields (QYs) and compared for the purpose of clarifying the differences between the pseudo-one-dimensional behavior and the pseudo-three-dimensional behavior of this type of copolymer. Finally, we discuss the PL QYs in relation to previously reported device characteristics so that we can gain insight into how copolymerization is related to the performance of optoelectronic applications.

2. Experiment

A detailed synthesis of fluorene-based statistical copolymers (PFTCVB*x*s) with low band-gap comonomers (TCVB) is described in [6]. The feed ratios of the TCVB for copolymerization were 1, 5, 10, 15 and 20 mol%. The average monomer molecular weights were calculated from the EHF and TCVB molecular weight values weighted by their ratio. The calculated effective monomer molecular weights of the corresponding PFTCVB*x*s (x = 1, 5, 10, 15, 20) are 390.0, 395.3, 401.9, 408.6 and 415.2, respectively. Solution samples for UV–vis and PL spectroscopy were prepared using a spectroscopic-grade chloroform solvent (99.9%, J. T. Baker, USA). The concentrations of the prepared solutions were approximately 1.7×10^{-2} wt% in chloroform. These mutual solutions were then diluted 100 times (1.7×10^{-4} wt%) for UV–vis and 1000 times (1.7×10^{-5} wt%) for PL to suppress re-absorption. In the case of the PFTCVB10 solution that was diluted 100 times, the concentration was 6.34×10^{-6} M as an effective monomer and 6.22×10^{-8} M as a polymer chain. Films of PFTCVB*x*s were spin-cast at 3000 rpm for 25 s with 150 μl of 0.8 wt% chloroform solutions. Before the spin-coating, we filtered the solutions by using a filter with a 0.2 μm pore size. The PFTCVB20 was warmed for 1 h at 50 °C because PFTCVB*x*s with a higher TCVB ratio have poor solubility in chloroform. The obtained films had an homogeneous film quality and a thickness of approximately 100 nm as estimated with a conventional surface profilometer.

For the UV–vis spectra of the solutions, we used a commercial UV–vis spectrophotometer (Cary 100, Varian Inc., USA) with quartz cells (Hellma, Germany) having an optical path length of 10 mm at room temperature. For the PL spectra of the solutions, we used a luminescence spectrometer (LS-50B, PerkinElmer, USA) with fluorescence quartz cells (Hellma, Germany) having an optical path length of 10 mm at room temperature. The UV–vis measurements of thin films were taken with the same equipment used for the solutions under ambient conditions at room temperature. Several measurements of the PL spectra were made with a CCD spectrometer (AvaSpec-2048FT, Avantes, Netherland) and a custom-designed light source with a 75 W Xenon arc-lamp combined with a conventional monochromator, and we compared the results with the results obtained from an LS-50B luminescence spectrometer.

To calculate accurate PL QYs from the obtained PL data, we tried to keep all the measurement conditions and configurations the same to avoid any refractive index differences between measurements. Note also that instead of using an integrating sphere method, which is regarded as the most accurate PL QY measurement, we intentionally took direct PL measurements, especially for films. This direct approach enabled us to reduce instabilities which was observed as fluctuations in the QY values during the integrating sphere PL QY estimation. The instable fluctuation is attributed to the different wave-guiding paths and re-absorption facilities of different film qualities at the edge.

3. Results

3.1. UV–vis spectra of PFTCVBx solution samples and film samples

The obtained UV–vis spectra of the diluted chloroform solutions at room temperature are shown in Fig. 2. When TCVB ratio is increased, the bands centered at 3.35 eV (370 nm) decrease linearly whereas the bands centered at 2.82 eV (440 nm) increase linearly. This fundamental UV–vis characteristic is analog in the film samples shown in Fig. 3 as the normalized UV–vis spectra. Additionally, the energetically higher lying bands of the films show a marginal blue-shift of 0.018 eV from the solution to the film samples at a TCVB ratio of 1 mol%, whereas the energetically lower lying bands have a similar red-shift of nearly 0.013 eV. (For simplicity, we refer to the bands of UV–vis spectra centered at 3.35 eV and 2.82 eV in the solution and the film samples as the B-band and the R-band, respectively.) The linear TCVB concentration dependencies of the absorbance values at the B-bands and R-bands of the solution and film samples confirm the correlation between the B-bands and the EHF monomers and between the R-bands and the TCVB monomers.

The normalized UV–vis spectra in Fig. 3A and B show nonlinear blue-shifts of the B-bands when the TCVB ratio is increased in

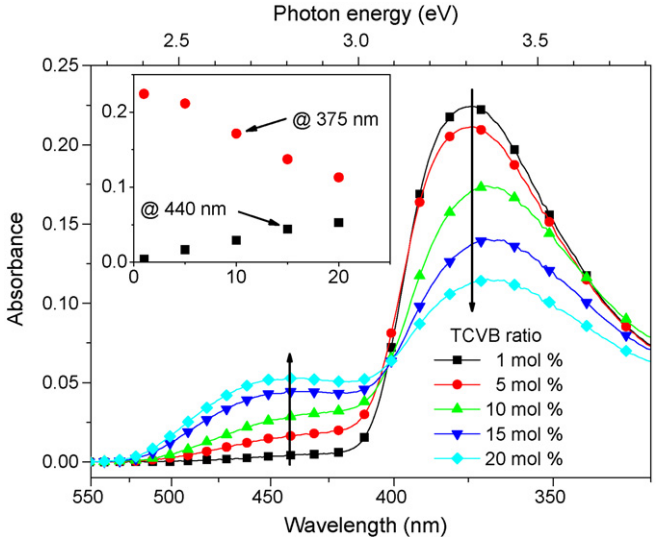

Fig. 2. UV–vis spectra of PFTCVB*x* solution samples. (*Inset*: plot of the absorbance maxima as a function of the TCVB ratio in mol%.)

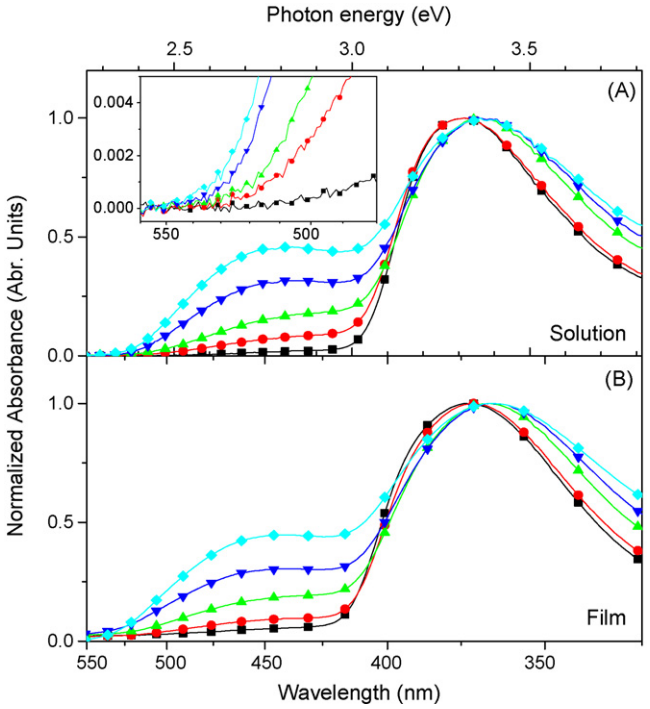

Fig. 3. Normalized UV–vis spectra of PFTCVB*x* as (A) diluted chloroform solutions and (B) spin-cast films. (Same symbols as in Fig. 2; *inset A*: magnification at the absorption edges of UV–vis spectra.)

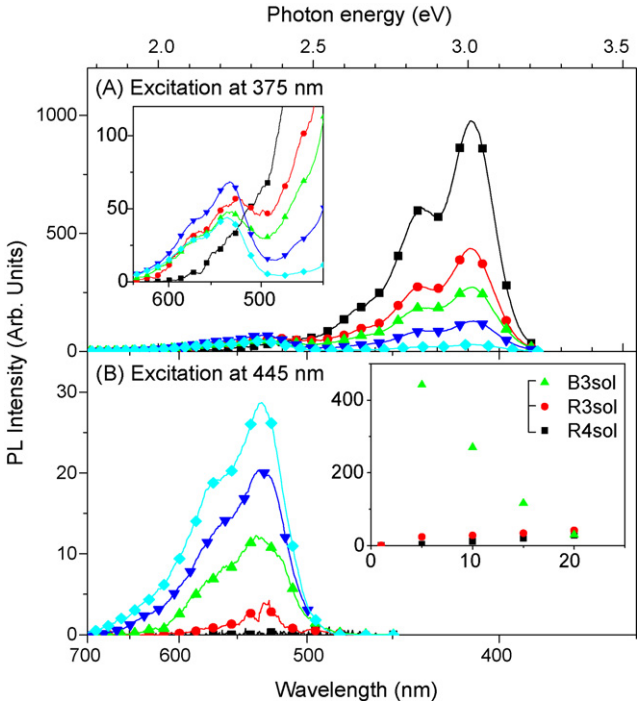

Fig. 4. PL spectra of PFTCVB*x* solution samples with excitation at (A) 375 nm and (B) 445 nm. *Inset A*: magnified PL spectra for the wavelength range of 450–650 nm; *inset B*: plot of PL intensity as a function of the TCVB ratio in mol%. (Same symbols as in Fig. 2.)

both the solution and film samples. There appears to be a type of stepwise transition at the TCVB ratio of 5–10 mol%, which is a sign of a significant change in the ground state of the electronic structure. These stepwise blue-shifts of the B-bands were 0.045 eV for both the solution and the film samples, though the blue-shifts of the films tend to be more gradual than those of the solutions. The half width at half maximum (HWHM) values of the B-bands for a TCVB ratio of 1 mol% are in the region of 0.194 eV and 0.241 eV for the solution and the film, respectively. The HWHM values of the R-bands at 20 mol% TCVB are in the region of 0.299 eV and 0.313 eV for the solution and film, respectively. The B-bands and R-bands both show a significant broadening of their HWHM values upon solidification. This trend may be a sign of increasing disorder due to the closely packed chains in the spin-coated thin films; the increasing disorder effect is caused by the stronger chromophore-to-chromophore interactions, which are typical of such randomly disordered solids as evidenced by the enhanced inhomogeneous broadening of the spectral bandwidths [10]. Moreover, a marginal but gradually increased HWHM was observed as the TCVB concentration increased in both the solution and film samples. Note also, as shown in the inset of Fig. 3A, that the R-bands have a red-shifting effect when the TCVB concentration is increased. This trend can be explained in terms of the change that occurs in the effective conjugation length when the TCVB ratio increases. The R-bands have a greater probability of extending the conjugation length when the TCVB concentration is increased, resulting in a red-shift of the R-bands. In contrast, the conjugation length of the B-bands should be shorter due to the increase in the number of TCVB comonomers on the chain. The effect of the conjugation length can be compared with a similar trend involving model oligomeric fluorenes [11].

3.2. PL spectra of solutions and films

While both emission bands with a PL maxima at 3.02 eV (410 nm) and 2.34 eV (530 nm) can be observed by excitation at 375 nm, only one emission band with a PL maxima in the region of 530 nm can be observed by site-selective excitation at 445 nm. (These PL emission bands of solution samples are denoted as the B3sol-band, R3sol-band, and R4sol-band, respectively; and the film PL spectra are denoted as the B3f-band, R3f-band, and R4f-band, respectively.) This site-selective result implies that the R-band is clearly related to the TCVB monomers, as indicated by the UV–vis spectra in Fig. 2. In the inset of Fig. 4B, the PL intensity maxima of the B3sol-band, R3sol-band and R4sol-band are plotted as a function of the TCVB ratio. The plots show linear dependence on the TCVB concentration. However, more than 90% of the PL intensity at the B-band decreases when the TCVB ratio increases from 5 mol% to 20 mol%, whereas the increase in the R-band intensity is not as rapid as the increase in the TCVB ratio. Nonetheless, this increasing trend appears linear.

A comparison of this enhanced decreasing of PL to UV–vis trend suggests the occurrence of additional TCVB-induced PL quenching of the B3sol-band. This quenching may be a relatively fast event because an exciton generated on a B-band can only move in a one-dimensional direction in a good solvated and diluted solution. This feature can be explained in terms of a Förster-type resonant energy transfer (FRET) because the overlap of B3sol emission bands with an R absorption band is almost perfect. Simultaneously, an electron-transfer-driven exciton dissociation and subsequent non-radiative recombination on the chain can be assumed [12]. Moreover, an extended conjugation length on this type of π-conjugated system can accelerate exciton migration to certain quenching centers. The experimental evidence for this type of enhanced quenching on a single π-conjugated molecule has been characterized in single-molecule spectroscopy studies as “blinking” [13]. Furthermore, there is a well-known example of a copolymer system consisting of fluorene and fluorenone monomers, though this system is mostly the result of inadvertent copolymerization due to photochemical oxidation [14]. These trends are discussed as absorbance-normalized PL QYs later in the discussion section of this study. Normalization of the PL spectra of the solution samples (though

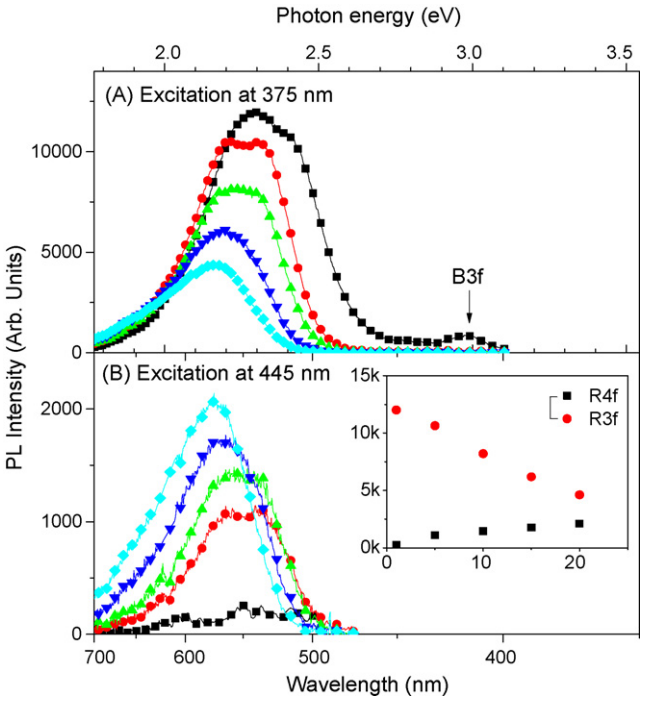

Fig. 5. PL spectra of PFTCVB*x* film samples with excitation at (A) 375 nm and (B) 445 nm; *inset*: PL intensity (arbitrary units) as a function of the TCVB ratio in mol%. (Same symbols as in Fig. 2.)

graphs are not shown here) reveals virtually no changes in any of the B3sol-band, R3sol-band and R4sol-band shapes or spectral dependences when the TCVB ratio is increase.

The PL spectra of the PFTCVB*x* film samples are shown in Fig. 5, and the PL maxima as a function of the TCVB ratio are shown in the inset of Fig. 5B. One of the most important differences between the film PL spectra and the solution PL spectra is that the B3f-band in the former is almost completely quenched at a TCVB ratio of 1 mol%. This feature is very close to the results of an earlier study that reports on the effective PL quenching of a poly-phenylenevinylene (PPV) derivative via doping with electron scavenging trinitrofluorenone [15].

Additionally, the R3f-band and the R4f-band are significantly red-shifted when the TCVB concentration is increased. To compare the band positions more accurately, we measured and compared the frontal edge energy values at their half maxima. This value for 5 mol% and 20 mol% TCVB films was 2.42 eV and 2.29 eV, respectively. To understand why the red-shift is pronounced in the film samples, we need to take into account the more extended degrees of freedom for the exciton diffusion due to the densely packed system [16]. An additional aspect may be re-absorption due to the R-bands that also have a red-shifted band edge down to approximately 530 nm when the TCVB ratio is increased.

Additional differences between the solution and the film samples include the disappearance of vibronic fine structures with an energy gap of approximately 0.18 eV, which is typical for a C=C double bond stretching mode, and the broadening of the full width at half maximum of the films (that is, 2.28 eV for solutions and 2.34 eV for films). On the other hand, the intensities of the B3f-band and the R3f-band decrease and the intensity of the R4f-band increases linearly with the TCVB concentration in a manner similar to that of the solutions, though the situations were moderately different.

4. Discussion

4.1. Exciton dissipation: solution versus film

Before starting the discussion on the PL QYs that were converted from the experimental PL data, we present a schematic energy level diagram with some initial remarks to avoid possible confusion due to the complexity of copolymeric systems. As shown in Fig. 6 and in other spectroscopic data, PFTCVB systems can be considered as copolymers with two dominate subsets of optically active sites: specifically, R and B sites. These two types of subsets should be related to the fluorene-rich sequences and TCVB-rich sequences as a general consequence of such statistical copolymerization. Furthermore, depending on their physical phase, the two types should be clearly distinguished in terms of a pseudo one-dimensional system in a solution consisting of a large amount of suppressed inter-chain interactions and a pseudo three-dimensional system in a film where there is pronounced inter-chain interactions due to the nature of the condensed phases.

As shown in the PL spectra, the TCVB-ratio-dependent PL quenching tendency of the solution samples is moderate whereas that of the film samples is highly efficient (>90% PL quenching from B* at 1 mol% of TCVB). An important reason for the suppressed PL quenching of the solution samples is related to the dimensional limitation of the exciton mobility due to the pseudo-one-dimensional π-conjugation along the polymer chains. For quantitative discussion of this tendency, the PL QYs of the solution and the film samples with various TCVB ratios are calculated and plotted in Figs. 7 and 8 as a function of the TCVB ratio. To calculate the PL QYs, we normalized the PL spectra excited at their B-band and R-band maxima by using their corresponding absorbance values and photon energies at the excitation wavelengths. We then scaled the obtained relative PL QYs by comparing the PL QY value of poly-fluorene (PF)

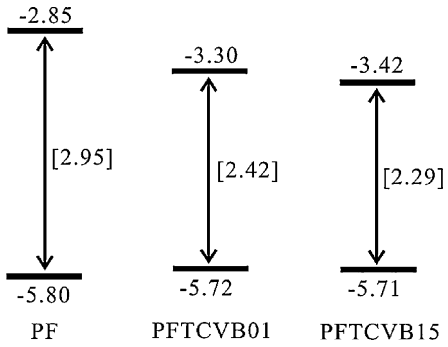

Fig. 6. Energy level diagram of relevant polymeric systems.

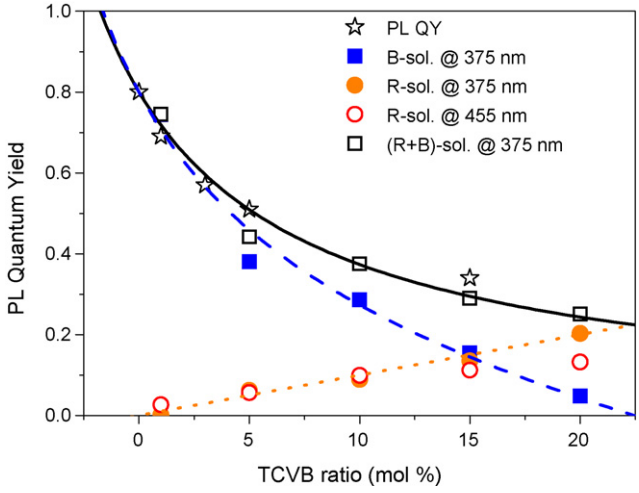

Fig. 7. PL QYs as a function of the TCVB ratio in mol% (PL QY: data from [6]).

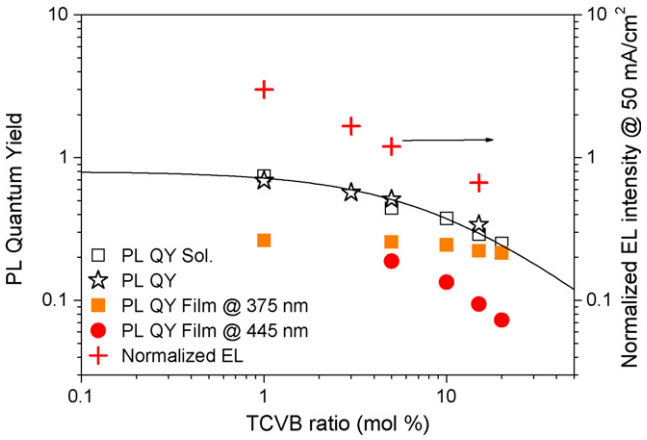

Fig. 8. PL QYs and normalized EL intensities as a function of the TCVB ratio in mol%.

without TCVB comonomers by using the previously reported PL QY value of 0.80 [6]. The selected excitation wavelengths were typically 3.31 eV (375 nm) and 2.79 eV (445 nm) for both the solution and film samples.

As shown in Fig. 7, the previously reported PL QY (open rectangles) of a solution at a given TCVB ratio can be coincidently reconstructed via the summing (B + R) (open rectangles) of its corresponding B3sol-band (rectangles) and R3sol-band PL QY (circles). This capability indicates that the PL QYs of the R3sol-bands are not dynamically populated by exciton migration. Rather, as shown in a previous study [6], they are the result of a direct population at their sites because the 2,5-bis(2-(5′-bromothienyl)-1-cyanovinyl)-1-(2″-ethylhexyloxy)-4-methoxybenzene comonomer also has an intensive UV–vis absorption band near 3.31 eV.

It is noteworthy that the PL QY trends of the R3sol-band and the R4sol-band are ostensibly similar. However, the PL QY trend of the R4sol-bands via direct excitation (open circles) should have constant QY values independent of the TCVB ratio unless there is specific chromophoric interaction when the TCVB ratio increases, which may suppress non-radiative decay of the exciton on the R-bands. In fact, the R4sol PL QY values converge to a PL QY value of approximately 0.15, whereas the R3sol values increase as the TCVB concentration increases. On the other hand, for the PL QY trend of the R3sol-band via the indirect population (circles), the linearly increasing tendency is understandable because this PL QY is normalized not by the TCVB numbers but by the EHF numbers. As a result, this R3sol PL QY trend reflects mainly the ratio between the number of photo-generated excitons on the B-band and the number of emitted photons from the R-band's excitons being populated by the transfer from the B-band. Another contribution to the R3sol PL QY is the ratio between the number of direct populations via photon absorption at the higher band of R and the number of emissions from the R-band. This consideration implies that the PL QYs of the R3sol-bands include not only the mutual emissive nature of the TCVB but also the nature of the transfer from the primary excitons on EHF sites to the migrated excitons on TCVB sites. Although the R3sol QYs can include the contribution by excitons from the B-bands, the experimental data appear to show that the TCVB-induced transfer does not contribute to radiative recombinations but makes a significant contribution to non-radiative dissipation. In fact, when the TCVB fraction numbers are normalized, the PL QYs in the case of an indirect population recover a virtually constant dependence.

A comparison of the total PL QYs and separately estimated PL QYs reveals a moderate but significant TCVB-induced non-radiative dissipation channel of photo-generated excitons on the B-bands in solution samples. The intrinsic PL QY of the TCVB comonomers with covalently bounded EHF side comonomers is approximately 80% less than that of the PF without TCVB comonomers. By adopting a simple kinetic scheme for singlet excitons as described in [15], we can fit the curves as shown in Fig. 7. Note that the TCVB-induced exciton transfer time of films is approximately three orders of magnitude smaller than that of the solutions, implying that the TCVB-induced B* transfer is nearly 1000 times faster in a solid than in a solution.

4.2. Comparison of the PL QY and device efficiency

As shown in Fig. 5, the efficient TCVB-induced PL quenching of B3f was observed for the film PL measurements. This highly effective quenching behavior precluded any analysis of this effect within a TCVB ratio range of 5–20 mol%. In this range, the primary excitons on the B sites can be assumed to be either quickly dissipated to a ground state non-radiatively or populated to R* sites and subsequently dissipated on R* non-radiatively.

The behavior observed in this study can be compared to the results of previous works on PPV derivatives doped by electron-accepting trinitrofluorenone. The results of those works are described in terms of a fast electron transfer [15] or unexpected copolymerization due to keto defects on poly-fluorene chains (which are often analyzed in relation to energy transfer) [14]. The fact that this efficient quenching behavior could be caused by an exciton dissociative electron transfer may explain the relatively high efficiency of the alternating copolymer as a photovoltaic material [8]. Furthermore, the possibility that the neighboring fluorene and TCVB, specifically a molecularly heterojunctioned situation, can accelerate exciton dissociation may provide a molecular level explanation.

Fig. 8 shows the PL QYs of (B3sol + R3sol) (open rectangles), R3f (rectangles), R4f (circles) and normalized electroluminescence (EL) intensities (crosses) of PFTCVB*x*s as a function of the TCVB ratio. While the solution sample with a TCVB ratio of 1 mol% has a PL QY value of approximately 0.7, its corresponding film sample has a TCVB ratio in the limited region of 0.25. Moreover, the trend of R3f PL QYs as a function of the TCVB ratio is mostly constant over the entire range of the measured TCVB ratio. Additionally, the trend of R4f PL QYs by direct excitation shows significantly decreasing behavior as the TCVB concentration increases. The R3f and R4f behaviors confirm that there is an additional quenching channel in film samples being pronounced with an increase in the TCVB ratio while there is no comparable quenching channel for the solution samples. Interestingly, the decrease of PL QYs with an increasing TCVB ratio is more pronounced in R4f than in R3f, whereas, in the corresponding trends of the solutions, R3sol and R4sol both show a marginal difference in their TCVB concentration dependences. This difference is a sign that the exciton population of R3f via an indirect population is significantly different to that of R3sol due to the significantly different physical phase situations, particularly diluted solutions and densely packed films.

As with the effective PL quenching of B3f, R4f also shows TCVB-ratio-dependent quenching behavior, a phenomenon that did not exist in the trend of the R4sol PL QYs. Unfortunately, this quenching behavior is not easily understood with the proposed simple scheme (Fig. 6), which relies on FRET or an electron transfer from R* to B*. Despite the fact that the process from R* to B* is an energetic uphill process, there is no overlapping of the donor emission and acceptor absorption bands that are necessary in the application of the FRET framework. Moreover, as shown in Fig. 8, the proper energy levels that are suitable for electron transfers are also absent. This situation is actually optimum for exciton confinement because it prevents unnecessary exciton diffusion and improves device efficiency [17]. One possible explanation is that when the TCVB concentration increases there is a stronger exciton dissociation and subsequent

non-radiative recombination due to a TCVB-induced energetic disorder effect similar to the inadvertent trapping of dopants [18].

With the HWHM broadening of the UV–vis spectra, the density of states (DOS) has been shown to expand to approximately 0.1 eV when copolymers with a higher TCVB ratio are cast from the solutions. This broadening of the DOS can be used to interpret the electrochemical values in Fig. 6, which were obtained from the solutions via conventional cyclovoltametry. This type of UV–vis broadening is known to change the DOS shape from Gaussian to a more extended exponential shape; thus, the increased sites at the tail parts of such DOS situations can act as self-traps [19].

As reported previously [6], the applied voltages were decreased from 6.2 to 1.42 V while the EL efficiencies were increased from 4 cd/m^2 to 10 cd/m^2 when the TCVB ratio was increased at the same current density of 50 mA/cm^2. This earlier behavior can be easily explained in terms of the reduction of the LUMO values that are compared in Fig. 8 and by the increasing number of TCVB sites on the PFTCVB chains when the TCVB ratio increases. More TCVB sites on the chains indicate, firstly, that more favorable channels exist for electron injections at the interface between the copolymer layer and, secondly, that the LiF/Al electrode has a higher work function than that of PFTCVB systems [20].

To compare the obtained PL QYs with the EL intensity data of PFTCVB*x*s, we collected the EL intensity values at the same current density of 50 mA/cm^2 and assumed that the electric exciton forming probability was identical under the same current density. Additionally, the EL intensity data were normalized by the number of TCVB ratios when the PL QYs were normalized by the corresponding absorbance; the purpose of this normalization was to maintain consistency in spite of the many other factors that can affect the EL efficiency [21]. In a comparison of the PL QYs of the film samples and the normalized EL intensities, we found that the normalized EL and particularly the R4f PL QYs have fairy close functional dependences when the TCVB concentration increases. From this comparison and from the information regarding the energy levels in Fig. 6, we can make the following observations about the EL situation in the PFTCVB*x*s copolymeric film systems: firstly, the charge carrier transport occurs mainly via TCVB sites, as shown by the decrease of the injection behaviors when the TCVB ratio increases [22]; secondly, the subsequent exciton formation via the electron and hole recombination takes place mainly on R* sites due to their narrower band-gap and especially because they have a lower LUMO and higher HOMO than the major EHF-based sites; and, thirdly, the EL emission finally occurs from the R* states with the same functional dependence as R4f PL QYs in Fig. 8.

5. Conclusion

In this study, we used time-integrated UV–vis and PL spectroscopy to characterize the exciton dissipation behaviors of fluorene-based π-conjugated statistical copolymers with narrow band-gap comonomers, TCVBs, with a wide feed ratio range of 1–20 mol%. From those spectroscopic data in both solution and film samples, we calculated the PL QYs as a function of the TCVB ratio and used the results to compare the different exciton dissipation behaviors of the solution and film samples in relation to the increase of the TCVB ratio. Finally, we discussed the TCVB concentration dependence of PL QYs in the film samples in terms of previously reported EL efficiencies of PFTCVB*x*s devices.

Our results confirm that the total PL QYs of the solution samples can be constructed by the summing of site-selectively estimated PL QYs for crucial subsets of the B-band and R-band. A comparison of the TCVB comonomer ratio dependences of PL QYs for both the solution and film samples the occurrence of moderate PL quenching of the B3sol-bands in the solution samples when the TCVB concentration is increased as well as significant enhancement of the PL quenching of the B3f-bands in the film samples. The obtained time constant for these PL quenching characteristics in the film samples, where very pronounced inter-chain interactions occurred, is approximately three orders of magnitude faster than that of the solutions. Furthermore, additional PL quenching of the R4f-bands when the TCVB ratio is increased was confirmed in the film samples; in contrast, we observed virtually no quenching of the R4sol-bands in the solution samples, where no significant inter-chain interactions occurred. Thus, the enhanced disorder within the films due to serious inter-chain interactions caused by close random packing is a plausible reason for the observed behavior.

Finally, we use the PL QYs of R4f as a function of the TCVB ratio to explain the quantitative relation between the EL efficiency and the TCVB comonomer ratio. A comparison of both the EL and PL functional dependences shows that the majority of charge carriers are transported through TCVB sites; it also shows that the excitons formed at the TCVB sites are radiatively dissipated when the excitons that photo-generate directly on the TCVB sites become relaxed to their mutual ground states.

Copolymerization is clearly an effective method of preventing unfavorable phase-separation in solid samples and of modifying homopolymer's unperturbed chemicophysical properties. However, the incorporation of additional functionality in the form of a different band-gap and different electrochemical potentials can lead to an unfavorable loss of excitons, especially because of the inter-chain interactions in the random solids. As shown in previous studies, this phenomenon is most likely beneficial for solar cell applications.

Acknowledgements

This work was supported by the Seoul R & BD Program and the Guest Associate Professor Program of the Nanoscience and Nanotechnology Center, Institute of Scientific and Industrial Research (SANKEN), Osaka University.

References

[1] J.H. Burroughes, D.D.C. Bradley, A.R. Brown, R.N. Marks, K. Mackay, R.H. Friend, P.L. Burn, A.B. Holmes, Nature 347 (1990) 539–541.
[2] J.B. Chang, V. Liu, V. Subramanian, K. Sivula, C. Luscombe, A. Murphy, J. Liu, J.M.J. Fréchet, J. Appl. Phys. 100 (2006), 014506/1–014506/7.
[3] Y. Yoshioka, G.E. Jabbour, Adv. Mater. 18 (2006) 1307–1312.
[4] J.E. Copenhafer, R.W. Walters, T.Y. Meyer, Macromolecules 41 (2008) 31–35.
[5] P. Prins, F.C. Grozema, F. Galbrecht, U. Scherf, L.D.A. Siebbeles, J. Phys. Chem. C 111 (2007) 11104–11112.
[6] N.S. Cho, D.-H. Hwang, J.-I. Lee, B.-J. Jung, H.-K. Shim, Macromolecules 35 (2002) 1224–1228.
[7] N.S. Cho, D.-H. Hwang, B.-J. Jung, E. Lim, J. Lee, H.-K. Shim, Macromolecules 37 (2004) 5265–5273.
[8] S.K. Lee, N.S. Cho, J.H. Kwak, K.S. Lim, H.-K. Shim, D.-H. Hwang, C.J. Brabec, Thin Solid Films 511 (2006) 157–162.
[9] M.M. Koetse, J. Sweelssen, K.T. Hoeker, H.F.M. Schoo, S.C. Veenstra, J.M. Kroon, X. Yang, J. Loos, App. Phys. Lett. 88 (2006), 083504/1–083504/3.
[10] H. Bässler, B. Schweitzer, Acc. Chem. Res. 32 (1999) 173–182.
[11] G. Klaerner, R.D. Miller, Macromolecules 31 (1998) 2007–2009.
[12] V. Arkhipov, E.V. Emelianova, H. Bässler, Chem. Phys. Lett. 340 (2001) 517–523.
[13] D.A. Vanden Bout, W.-T. Yip, D. Hu, D.-K. Fu, T.M. Swager, P.F. Barbara, Science 277 (1997) 1074–1077.
[14] E.J.W. List, R. Guentner, P.S. de Freitas, U. Scherf, Adv. Mater. 14 (5) (2002) 374–378.
[15] C. Im, J.M. Lupton, P. Schouwink, S. Heun, H. Becker, H. Bässler, J. Chem. Phys. 117 (2002) 1395–1402.
[16] C. Chi, C. Im, G. Wegner, J. Chem. Phys. 124 (2006), 024907/1–024907/8.
[17] B.D. Chin, C. Lee, Adv. Mater. 19 (2007) 2061–2066.
[18] C. Im, E.V. Emelianova, H. Bässler, H. Spreitzer, H. Becker, J. Chem. Phys. 117 (6) (2002) 2961–2967.
[19] V.I. Arkhipov, J. Reynaert, Y.D. Jin, P. Heremans, E.V. Emelianova, G.J. Adriaenssens, H. Bässler, Synth. Met. 138 (2003) 209–212.
[20] Y.D. Jin, X.B. Ding, J. Reynaert, V.I. Arkhipov, G. Borghs, P.L. Heremans, M. Van der Auweraer, Org. Elect. 5 (2004) 271–281.
[21] A.J. Campbell, D.D.C. Bradley, D.G. Lidzey, J. Appl. Phys. 82 (12) (2004) 6326–6342.
[22] R. Coehoorn, Phys. Rev. B 75 (2007), 155203/1–155203/10.